

WHOLESALE DEBRIS REMOVAL FROM LEO

Eugene Levin^a, Jerome Pearson^a, Joseph Carroll^b

^aStar Technology and Research, Inc., SC 29466, USA

^bTether Applications, Inc., CA 91913, USA

Abstract

Recent advances in electrodynamic propulsion make it possible to seriously consider wholesale removal of large debris from LEO for the first time since the beginning of the space era. Cumulative ranking of large groups of the LEO debris population and general limitations of passive drag devices and rocket-based removal systems are analyzed. A candidate electrodynamic debris removal system is discussed that can affordably remove all debris objects over 2 kg from LEO in 7 years. That means removing more than 99% of the collision-generated debris potential in LEO. Removal is performed by a dozen 100-kg propellantless vehicles that react against the Earth's magnetic field. The debris objects are dragged down and released into short-lived orbits below ISS. As an alternative to deorbit, some of them can be collected for storage and possible in-orbit recycling. The estimated cost per kilogram of debris removed is a small fraction of typical launch costs per kilogram. These rates are low enough to open commercial opportunities and create a governing framework for wholesale removal of large debris objects from LEO.

1. Introduction

Space debris from discarded upper stages, dead satellites, and assorted pieces from staging, tank explosions, and impacts has been growing since the beginning of the space age. There are currently about 9,000 tracked debris objects in LEO per 450 operational satellites (20 to 1 ratio), while the number of untracked lethal impactors in the centimeter range is simply staggering, on the order of 500,000. The risk to active satellites and the need for avoidance maneuvering have increased dramatically in the past few years [1].

Up until 2009, the dangers of space debris were generally ignored under the “big sky” theory, but the Cosmos-Iridium collision changed that. On February 10, 2009, a fully maneuverable and “well-behaved” operational satellite ran into a 16-year-old derelict satellite at 11.6 km/s. In less than a millisecond, the two satellites disintegrated, producing nearly 2,000 tracked debris objects and on the order of 100,000 untracked fragments in the centimeter range. This came as a sobering preview of things to come.

After years of debris accumulation, the LEO debris cloud has crossed critical density thresholds over a wide range of altitudes [2], as predicted by Kessler, and entered into a phase of accelerated debris creation in collisions that become more and more frequent. The collision rate scales with the second power of the density of large debris, which has grown nearly linearly over the last 50 years. In this deteriorating environment, a collision like Cosmos-Iridium was bound to happen, and the theory predicts that we may witness another catastrophic collision in this decade [2]. The Cosmos-Iridium collision involved a total mass of 1.5 tons, which was substantially less than the average mass statistically expected to be involved in a collision between intact objects. The next catastrophic collision is more likely to be on a scale comparable to the Chinese ASAT test and the Cosmos-Iridium collision combined.

The NASA Orbital Debris Program Office has been arguing for quite some time that in addition to debris mitigation we need to start removing at least 5 large objects per year to prevent the “debris runaway” or “Kessler Syndrome” [2]. This is the minimum rate required just to stabilize the current environment, which means still having catastrophic collisions every decade or so, but at least not more frequently. A recent study conducted for the International Academy of Astronautics suggested removing 10-15 large intact objects from LEO per year [3,4]. In 2011, the ESA Space Debris Office concluded that half-measures are not enough, and the goal should be to remove LEO debris en masse as soon as possible [1].

In this article, we will discuss some general relations and one practical implementation of the wholesale removal of large debris from LEO.

2. LEO debris ranking

The LEO debris environment is well characterized by models like ORDEM, MASTER, LEGEND, and others, even though there are some noticeable differences in their estimates of the number of small debris particles in certain regions [5]. There are three major groups of lethal debris objects in LEO. Using a highway analogy for illustrative purposes [6], we can say that satellites and stages are like cars, small components shed along the way are like hubcaps, but those hundreds of thousands of small fragments generated in “car” collisions are more like shrapnel, whizzing all around active satellites at orbital speeds (Table 1).

Table 1. Lethal Debris Objects in LEO

Type	Characteristics	Hazard
“Shrapnel”	Untracked, over ~ 1 cm, 98% of lethal objects	Primary threat to satellites; too small to track and avoid, too heavy to shield against
“Hubcaps”	Tracked, > 10 cm, < 2 kg, 2% of lethal objects	Most conjunctions and avoidance maneuvers for operational satellites
“Cars”	Tracked, over 2 kg, $< 1\%$ of lethal objects	Primary source of new shrapnel; 99% of the collision area and mass

Due to the large numbers, the “shrapnel” is the primary threat to operational satellites, and most new pieces will come from collisions involving “cars”, because the “cars” account for nearly all collision area and mass of the debris. This means that we must remove the old “cars” to prevent LEO pollution with more “shrapnel.” The collision-generated debris potential associated with large objects can be estimated by the statistically expected cumulative yield of fragments generated in catastrophic collisions,

$$R_k = M_k P_k, \quad (1)$$

where M_k is the mass of the debris object, and P_k is the probability of a catastrophic collision involving this object over a certain period of time. A risk measure of this kind has been also suggested by NASA [2, 7]. The probabilities P_k can be evaluated from the debris environment models or computed from the catalog with averaging over a representative period of time,

$$R_k = M_k \sum_n P_{kn}, \quad (2)$$

where P_{kn} are the probabilities of a collision between objects k and n , assuming that they are small enough to disregard event dependency. Collisions between “cars” are usually catastrophic, and even a very small “car” like a 4-kg 3U CubeSat can

smash a really large “car” into small pieces, especially in a head-on collision. The whole LEO debris cloud is dynamic, and the probabilities P_{kn} vary with time, as the orbits and population change. For example, after the Cosmos-Iridium collision, the corresponding terms P_{kn} dropped out of the probability matrix.

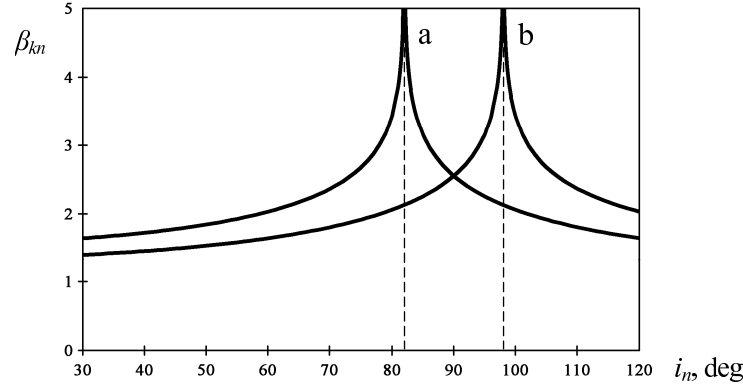


Fig. 1. Inclination pairing coefficient for $i_k = 98^\circ$ (a) and $i_k = 82^\circ$ (b).

An important feature of the probabilities P_{kn} is their sensitivity to “inclination pairing” observed when $i_k + i_n$ is approaching 180° . Fig. 1 illustrates this notion by plotting typical multipliers β_{kn} resulting from “inclination pairing,” as described in [6]. For objects at $i_k = 98^\circ$, the multiplier peaks at $i_n = 82^\circ$ (a), while for objects at $i_k = 82^\circ$, it peaks at $i_n = 98^\circ$ (b). This happens because the orbits at 82° and 98° precess in the opposite directions, and when they become nearly coplanar, the objects move head-on, greatly increasing the probability of collision. The implications are significant, as we will see below. One of the examples is that the satellites of the NASA Earth Observing System operating in Sun-sync orbits encounter a high percentage of head-on conjunctions [8].

We can now evaluate collision-generated debris potential of selected groups of debris objects,

$$R_g = \sum_{k,n} M_k P_{kn}, \quad (3)$$

and analyze its cumulative distributions by location and ownership. Fig. 2(a) shows the cumulative distribution of the collision-generated debris potential by 5° inclination bins compared to the distribution of the number of operational satellites in LEO (b) according to [9].

Three clusters stand out, $71\text{-}74^\circ$, $81\text{-}83^\circ$, and Sun-sync, of which the last two are “inclination paired,” as explained above, and represent elevated collision threats to each other. Removing just old upper stages from these three clusters would make a huge difference. The overall collision-generated debris potential would drop by a factor of 4. We will see later that this task could be accomplished by as few as four 100-kg electrodynamic vehicles in 7 years. Focus on the upper stages in the high inclination clusters was also suggested in [10].

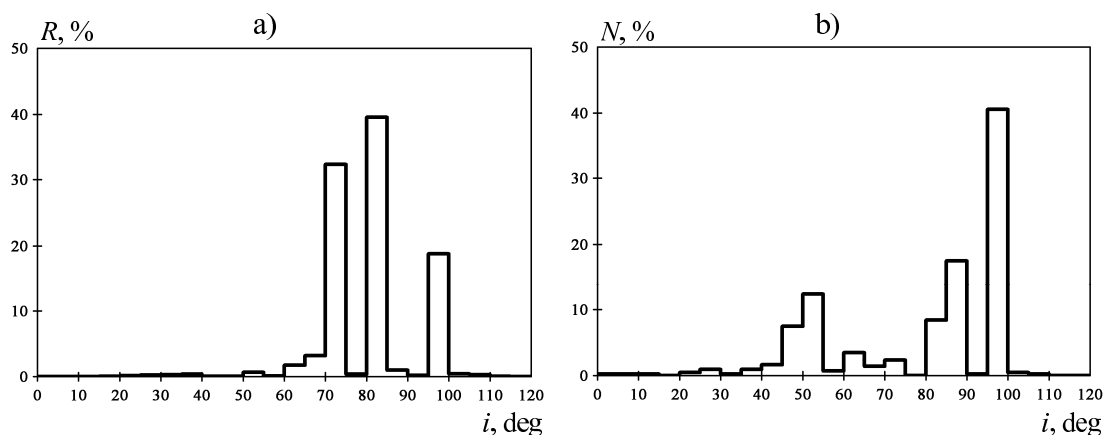


Fig. 2. Distribution of the collision-generated debris potential (a) and the number of operational satellites (b).

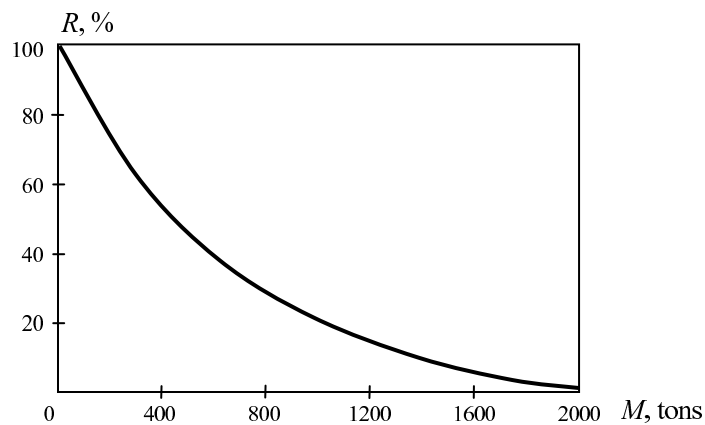


Fig. 3. Reduction of the collision-generated debris potential with removal of large debris objects.

Fig. 3 shows the impact of removing large debris. We see that only removal of hundreds of tons of large debris can make a noticeable difference in the collision-generated debris potential in LEO. When many objects are removed, the statistically expected frequency of catastrophic collisions will drop drastically as well.

In search of a workable solution for wholesale debris removal, we will consider drag devices, rockets, and specially designed electrodynamic vehicles.

3. Debris removal with drag devices

Drag devices (such as inflatables, solar sails, and hanging electrodynamic tethers) may work for some newly launched objects, but they are not well suited for wholesale debris removal. First of all, they have to be somehow delivered and attached to derelict objects, which may require a lot of propellant and hundreds of

delivery vehicles. What is not commonly recognized, they will introduce excessive mutual collision risks if used en masse because of their large collision areas.

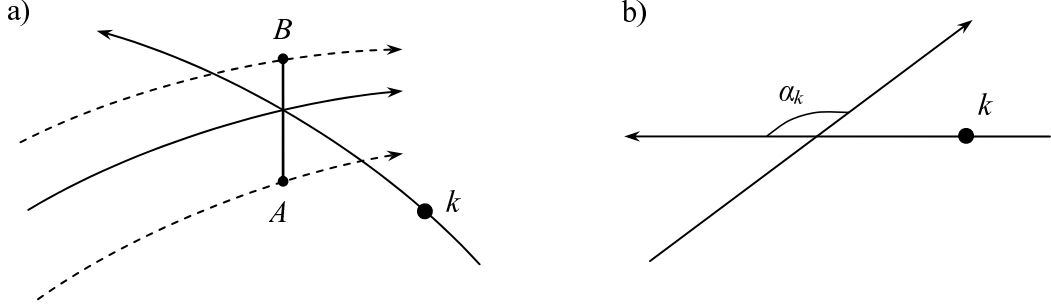


Fig. 4. Conjunction with a tether.

To get an idea of the collision risks involved, let us consider a model problem of deorbit runs with passive electrodynamic drag tethers in a cloud of a large number of objects in nearly circular orbits. Fig. 4(a) shows an electrodynamic tether AB deployed vertically from a large debris object B . As they slowly spiral down, the tether will cross multiple orbits of other objects. With random phasing and random orientation of the objects, the probability of running into object k at a given crossing can be estimated as

$$p_k \approx \frac{D_k}{2\pi R_k \psi_k}, \quad (4)$$

where D_k is the average linear dimension of the object, R_k is the orbit radius of the object, $\psi_k = \cos(\alpha_k/2)$ with $|\alpha_k| \leq \pi - 2\delta_k$, and $\psi_k = \delta_k$ with $\pi - 2\delta_k \leq |\alpha_k| \leq \pi$, while $\delta_k = D_k/\pi R_k$, and α_k is the conjunction angle shown in Fig. 4(b). Note that the probability of collision is the highest for head-on conjunctions, when $|\alpha_k| \rightarrow \pi$.

With a nearly vertical tether, the crossings will persist for $N \approx L/\Delta R_{tk}$ orbits, where L is the tether length, and ΔR_{tk} is the average altitude drop per orbit for the debris dragged down by the tether at the radius R_k . The same condition will be repeated on the opposite side of the orbit, doubling the probability of collision. Therefore, the cumulative probability of collision with object k can be estimated as $p_{kt} \approx 2p_k L/\Delta R_{tk}$.

The total probability of collision for the entire deorbit run is obtained by summation over all objects, whose orbits are crossed by the tether,

$$P_t \approx \frac{L}{\pi} \sum_k \frac{D_k}{R_k \Delta R_{tk} \psi_k}. \quad (5)$$

The multitude of possible realizations of the deorbit run will involve various relative positions of the ascending nodes due to the nodal regression and phasing of

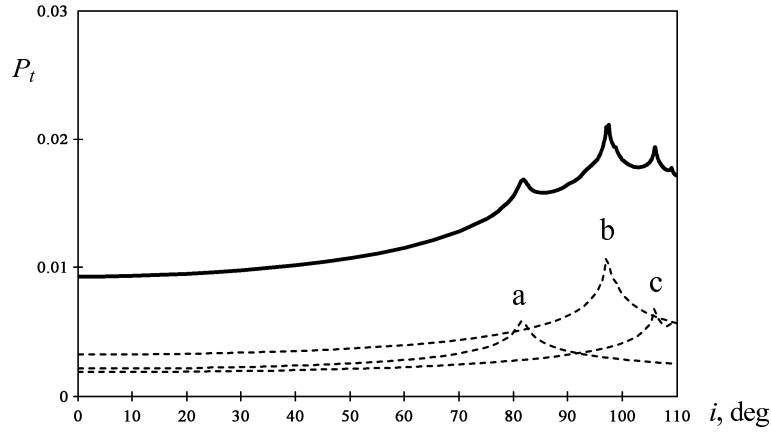


Fig. 5. Collision risk distribution for a passive electrodynamic drag tether and contributions from a) Sun-sync, b) 81-83°, c) 71-74° clusters.

the deorbit run segments. Averaging over the ascending node differences φ_{kt} yields

$$P_t \approx \frac{L}{\pi} \sum_k \frac{D_k \beta_{kt}}{R_k \Delta R_{tk}}, \quad \beta_{kt} = \frac{1}{2\pi} \int_0^{2\pi} \frac{d\varphi_{kt}}{\psi_k}, \quad (6)$$

where the multipliers β_{kt} reflect “inclination pairing” illustrated earlier in Fig. 1.

A typical distribution of the collision risk for a passive 10-km tether descending at a rate of 0.5 km/orbit is shown in Fig. 5. The peaks at high inclinations are due to “inclination pairing” with the objects in the Sun-sync, 81-83°, and 71-74° clusters, whose contributions to the overall risk are shown by dashed curves *a*, *b*, and *c*, respectively. It is clear now why passive electrodynamic drag tethers are not suitable for wholesale debris removal: with hundreds of them in orbit, collisions with large objects will be guaranteed.

Moreover, when multiple passive tethers are in orbit, their dimensions should be added to the sums in equations (5) and (6). With typical tether lengths comparable to the sum of dimensions of all cataloged objects in LEO, this will increase collision probabilities roughly in proportion to the number of tethers.

Similar formulas for inflatables and solar sails show signs of the same problem: they would become substantial collision hazards if deployed in large numbers. These added risks would require active mitigation, which may be challenging by itself.

4. Debris removal with rockets

To understand requirements and limitations of this approach, let us consider a simplified problem of moving K debris objects M_1, M_2, \dots, M_K from circular orbits at altitudes H_1, H_2, \dots, H_K to circular orbits at a lower altitude H_0 . The migration will be attempted by N tugs with a dry mass m_0 and fuel capacity m_f . Let us

disregard the penalties for the inclination and node changes and assume that all tugs are placed in orbits with the same inclination as their targets, and that the differential nodal regression is used to match the nodes. Let us also assume that the tugs have low thrust engines with a specific impulse I_s .

Each tug will start at an altitude H_0 and spiral up to its next target M_j at an altitude H_j , capture the target, and then spiral back down to the altitude H_0 , where the debris will be released for natural decay. We will approximate the delta-V for the transfer between the two orbits as

$$\Delta v_j \approx \frac{1}{2} \omega (H_j - H_0),$$

where ω is a fixed orbital angular rate. The amount of fuel consumed on this round trip will be approximated as

$$\Delta m_{fj} \approx (m_{tu} + m_{td} + M_j) \frac{\Delta v_j}{I_s g},$$

where m_{tu} and m_{td} are the average masses of the tug on the way up and down, and g is gravity. Statistically, with many trips, the tugs will be carrying half of the fuel on average, and we will use an average value of $2m_0 + m_f$ instead of $m_{tu} + m_{td}$ for the purpose of summation. Then, the total amount of fuel consumed in the process of migration will be

$$M_f = \sum_j \Delta m_{fj} \approx (2m_0 + m_f) K \varkappa_a + M_d \varkappa_m, \quad (7)$$

where

$$\varkappa_a = \frac{\omega}{2I_s g} (H_a - H_0), \quad \varkappa_m = \frac{\omega}{2I_s g} (H_m - H_0),$$

M_d is the total mass of the debris objects, and H_a and H_m are their simple and weighted altitude averages,

$$M_d = \sum_j M_j, \quad H_a = \frac{1}{K} \sum_j H_j, \quad H_m = \frac{1}{M_d} \sum_j M_j H_j.$$

Substituting $m_f = M_f/N$ into (7), we find the total mass of fuel, and then, the total mass of the tugs with fuel

$$M_t = Nm_0 + \frac{N}{N - K \varkappa_a} (2m_0 K \varkappa_a + M_d \varkappa_m). \quad (8)$$

The total mass of the tugs is the lowest when the number of tugs is equal to

$$N = K \varkappa_a (1 + \sqrt{2 + \psi}), \quad (9)$$

where

$$\psi = \frac{M_a (H_m - H_0)}{m_0 (H_a - H_0)}, \quad M_a = \frac{M_d}{K}.$$

Here, M_a is the average mass of the debris objects. The total amount of fuel and the total mass of the tugs with fuel are equal to

$$\begin{aligned} M_f &= M_d \kappa_m \frac{1}{\psi} (2 + \psi + \sqrt{2 + \psi}), \\ M_t &= M_d \kappa_m \frac{1}{\psi} (3 + \psi + 2\sqrt{2 + \psi}), \end{aligned} \quad (10)$$

while the amount of fuel per tug is equal to

$$\frac{m_f}{m_0} = \frac{2 + \psi + \sqrt{2 + \psi}}{1 + \sqrt{2 + \psi}}, \quad (11)$$

and the average number of debris objects removed per tug is equal to

$$\frac{K}{N} = \frac{1}{\kappa_a (1 + \sqrt{2 + \psi})}. \quad (12)$$

For bi-propellant, it is possible to deorbit debris by lowering the perigee to some altitude H_p that guarantees quick reentry. In this case, the required delta-V is approximated as

$$\Delta v_j \approx \frac{1}{4} \omega (H_j - H_p),$$

and formulas (9)–(12) apply with

$$\kappa_a = \frac{\omega}{4I_s g} (H_a - H_p), \quad \kappa_m = \frac{\omega}{4I_s g} (H_m - H_p), \quad \psi = \frac{M_a (H_m - H_p)}{m_0 (H_a - H_p)}.$$

With a given ψ , the number of tugs is proportional to the number of debris objects, while the masses of fuel and the tugs are proportional to the total mass of the debris, and all values are inversely proportional to the specific impulse. The number of tugs grows with ψ , but their total mass drops. Because ψ is inversely proportional to the dry mass m_0 , making m_0 as small as possible reduces the total mass. However, it also reduces the amount of fuel per tug, according to (11), which may become insufficient for moving large objects.

Fig. 6 shows the total mass and the number of tugs optimally required to remove all LEO debris over 2 kg as a function of the specific impulse of the propulsion system. The tug dry mass is set to $m_0 = 100$ kg. The dots on the left represent the bi-propellant solutions with $H_p = 80$ km, while the lines represent the high-Isp solutions with $H_0 = 330$ km. We see that low-Isp systems would require excessive

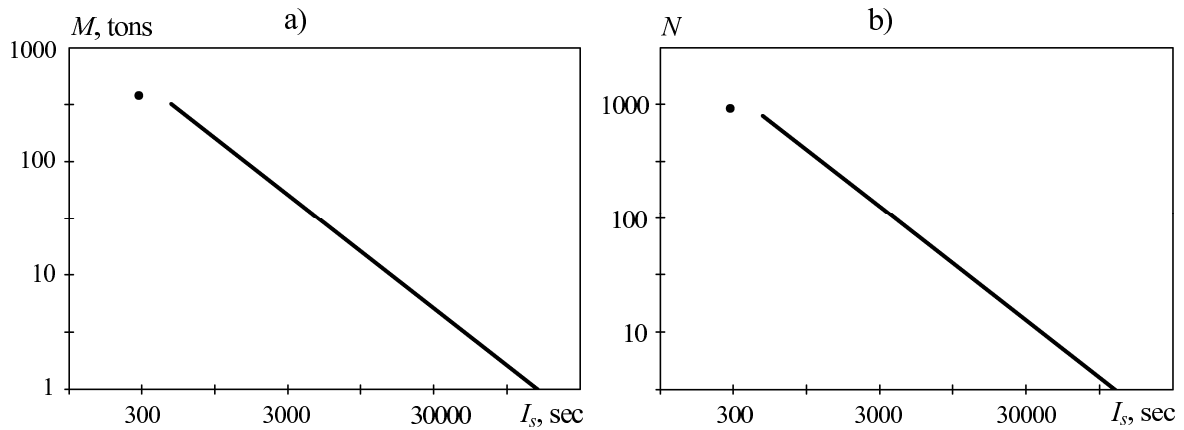


Fig. 6. Total mass (a) and number of tugs (b) for wholesale debris removal.

mass and number of tugs, while cost-effective solutions would require Isp's much higher than currently available. Some economy promised by bi-propellant fuel depots is not that impressive for this particular task and is offset by higher complexity of the design and operation.

5. Electrodynamic system for debris removal

Today, electrodynamic propulsion is the only candidate that can meet the high Isp requirements discussed in the previous section and provide thrust at a newton level, while being very economical and lightweight.

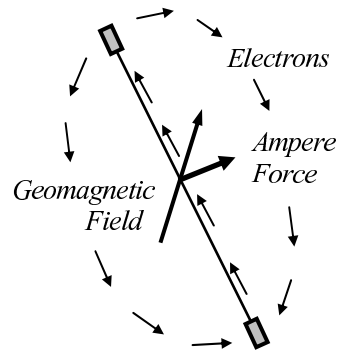


Fig. 7. Electrodynamic propulsion.

The electrodynamic thrust is the Ampere force acting on a conductor in the geomagnetic field (Fig. 7). Electrons are collected from the ambient plasma on one end and emitted back into the plasma from the other end. The current loop is closed through the ionosphere. Electron collection can be achieved by biasing bare metal surfaces, while the most efficient electron emission devices in the ampere range are hollow cathodes. They spend a small amount of xenon. Taking into account

this expenditure, the equivalent Isp of the electrodynamic system described later in this section is on the order of 200,000 sec. This places it far on the right on the performance charts in Fig. 6 and makes it a leading candidate for wholesale debris removal in terms of performance.

The electrodynamic propulsion technology is not new – it has been in development for over 25 years. The first demonstration in orbit took place in 1993 during the Plasma Motor Generator experiment by NASA Johnson. It used insulated copper wire and hollow cathodes on both ends for electron emission and collection. PMG was the second in the series of four successful flights with J. Carroll's tethers and deployers that included also SEDS-1 in 1993, SEDS-2 in 1994, and TiPS in 1996.

In 1996, TSS-1R demonstrated effective bare surface electron collection, ionospheric circuit closing with emission nearly 20 km away from the collection area, and revealed the arcing problem at high voltages.

In 1998-2002, NASA Marshall designed and built the Propulsive Small Expendable Deployer System (ProSEDS) to demonstrate electrodynamic de-orbit of a 1-ton Delta II upper stage. J. Carroll designed the tether and the deployer. The system involved 500 m of insulated wire, 4.5 km of bare aluminum wire, and a 10-km non-conducting "pilot" tether, with a 20-kg counterweight at the end. The flight was delayed and then canceled due to changing perspectives on risks to ISS after the Columbia accident. It would have been the first debris removal mission with an electrodynamic tether.

In 1999-2000, J. Carroll designed and built the Mir Electrodynamic Tether System (METS), and E. Levin provided dynamic analysis and flight control algorithms [11, 12]. The tether consisted of a 6-km insulated wire, 1-km bare aluminum tape for electron collection, and a 0.5-km pilot tether. A spare 200-kg Manned Maneuvering Unit was to be attached in orbit as a counterweight. The system would draw 2 kW of power from Mir and produce 0.2 N of average thrust along track to keep Mir in orbit without fuel re-supply, allowing the newly formed MirCorp to open Mir to commercial space tourists. Unfortunately, the decision was made to deorbit Mir before there was a chance to test METS.

A radical departure from the previous designs occurred in 2001, when E. Levin suggested spinning to improve stability and widen the range of angles with the geomagnetic field, and J. Carroll designed the first spinning electrodynamic tether system. It featured multiple distributed power nodes to reduce voltages and prevent arcing (a lesson learned from TSS-1R) and bare aluminum tapes for the full tether length to improve performance at low plasma densities, provide more flexibility of control, and greatly increase tether survivability [11–13]. The design was matured and tape prototypes were manufactured and tested under SBIR contracts with the AFRL. The work resulted in major improvements in performance and reliability characteristics of electrodynamic systems.

Electron collection with a bare aluminum tape was tested by JAXA in August 2010, when a tape 133 m long and 25 mm wide was deployed from a suborbital rocket [14]. JAXA has an ongoing research program on active debris removal with electrodynamic tethers [15].

In recent years, the Naval Research Laboratory took the initiative of advancing the electrodynamic propulsion technology and is currently building a 3U CubeSat for the Tether Electrodynamic Propulsion CubeSat Experiment (TEPCE) [16, 17]. The 1.5U end-bodies will be energetically separated by a stacer spring, deploying a 1-km conductive tether. The system will demonstrate electron emission and collection, electrodynamic propulsion, tether libration control, orbit determination and navigation. In addition, it will collect plasma measurements over a wide range of ionospheric conditions. J. Carroll and E. Levin are contributing to the TEPCE design and analysis.

The current design layout of the spinning electrodynamic system is shown in Fig. 8. It includes two end-bodies with the controllers and electron emitters, and multiple power nodes with the primary solar arrays, all connected sequentially with reinforced bare aluminum tapes. The tapes are 1 km long, 30 mm wide, and 0.04 mm thick, and serve both as conductors and electron collectors. A 10-section vehicle weighs only 100 kg, including 41 kg of tape, 3 kg in each power node, and 16 kg at each end. Two vehicles will fit into one ESPA slot [18].

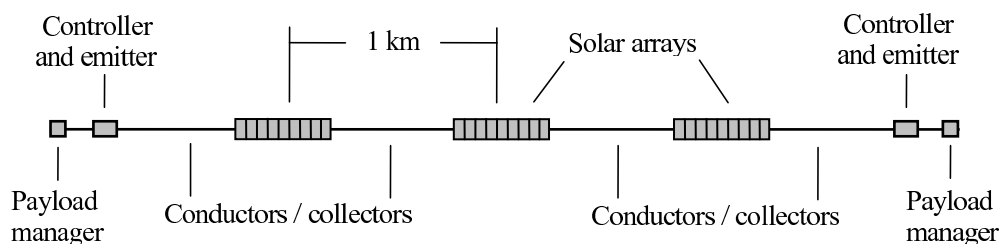


Fig. 8. Design layout of the spinning electrodynamic system.

The vehicle is highly redundant and survivable. Propellantless thrust and on-board GPS allow avoidance of all tracked objects by wide margins. The tapes are immune to punctures by small particles in the millimeter range and smaller. The probability of a tape cut by untracked debris in the centimeter range is much lower than a typical probability of failure of the spacecraft avionics. Even if the tape is cut, both parts remain controllable and can deorbit themselves in days, avoiding all other objects.

The entire structure rotates slowly at 6-8 revolutions per orbit. This gives stability and better angles between the conductor and the geomagnetic field, especially in high inclination orbits. All orbital elements, as well as the tether orientation and vibration, can be controlled by varying and reversing the currents in different sections of the conductor [12]. Each inboard node produces about 0.8 kW of power,

and the vehicle can make large orbit changes in a fairly short time. In deboost mode, additional energy can be extracted from the orbital motion through the emf, substantially increasing the thrust capability. Being propellantless, the vehicle is not limited by the Tsiolkovsky rocket equation and can produce enormous delta-Vs of hundreds of km/sec over its operational lifetime.

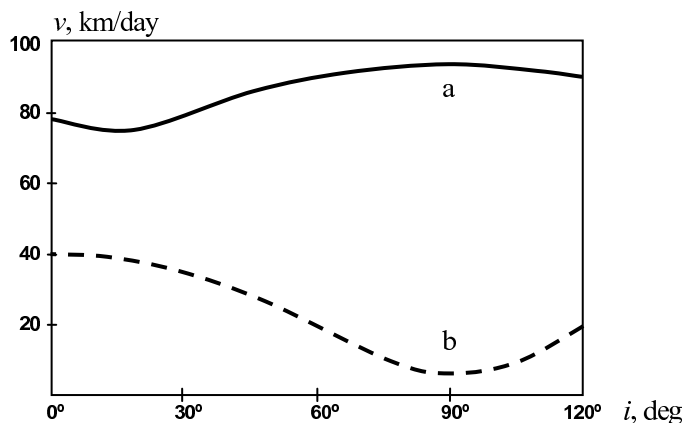


Fig. 9. Deorbit rate of the spinning (a) and vertical (b) electrodynamic tether systems with 1-ton object.

Fig. 9 compares altitude rates of the spinning system (a) and a conventional vertically oriented system (b) dragging down a 1-ton object. The difference is drastic, especially at high inclinations, where most of the large debris is concentrated. There are two reasons. First, for a vertical electrodynamic system to remain stabilized and controllable, the thrust must be an order of magnitude less than the tension produced by the gravity gradient, while the spinning system can apply all the thrust it is able to produce electrically [12]. Second, a vertical system cannot produce much of a thrust along-track in near-polar orbits because of the orientation of the geomagnetic lines, while the spinning system can spin normal to the orbital plane and get very good “traction” with the geomagnetic field.

According to formulas (5)–(6), high descent rates greatly reduce the exposure to the risks of collision with other objects, because their orbits are crossed in much shorter time, especially at high inclinations. At the same time, active avoidance of all tracked objects is the key to alleviating general concerns about the risks of tether operations in LEO [19, 20]. With its high and persistent maneuverability, the spinning electrodynamic system is fully capable of meeting this requirement.

For debris removal, the payload managers at each end carry many large, lightweight nets (~ 50 g each). To catch a debris object, the orbit is matched with the target, a net is extended from the payload/net manager by the centrifugal force at the end, the target is approached at a few meters per second under manual control from the ground, the net is enclosed around the target, and the transient dynamics is damped out, even if the object is tumbling up to 1–2 rpm. Most old

debris objects are expected to rotate much slower, due to eddy-current damping in their aluminum structure [21, 22]. Fig. 10 illustrates schematically how the restoring torque is applied to the debris object. The tether tension T_t is induced by the rotation of the entire system, while the tension T_n in the net straps reacts to the rotation of the debris object. If the capture approach was not successful, it is repeated. Multi-kilometer-base binocular vision from cameras on the end-bodies or nodes is used to assist the approach. Some prototype nets were tested during the NIAC study on debris removal [23], and improved net and net manager designs are in development.

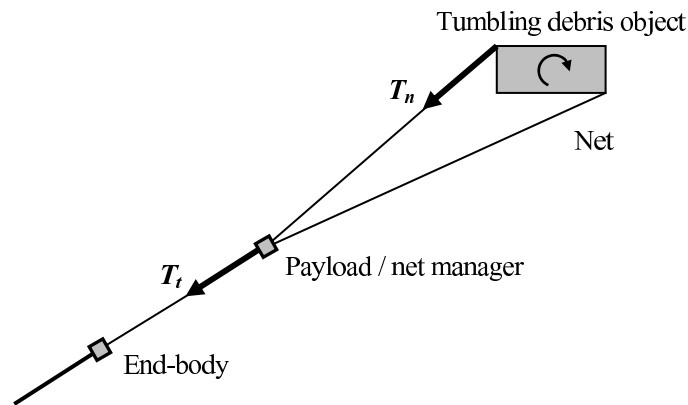


Fig. 10. Automatic detumbling during the net capture with the spinning system.

Substantial benefits are inherent in this capture method compared to what can be done with free-flying tugs. The tugs cannot use nets or lines, because they will wrap around the tumbling object and pull the tug in. They must approach and literally “land” on the tumbling object, avoiding appendages, and attach themselves within seconds, or the object will swing the “lander” away. This is very risky, particularly, for electric tugs with large solar arrays, and has to be done differently for different objects. Even when attached, pushing the object toward deorbit destabilizes its attitude and will require complex balancing.

By contrast, the electrodynamic vehicle does not come closer than 20–50 m, and only a light disposable net is extended into the vicinity of the object, while the solar arrays and other parts are stabilized by rotation at safe distances from the debris object. The multi-newton tension in the net induced by the rotation of the entire system rapidly synchronizes the object’s rotation with the tether rotation without any special control and continues to hold the object firmly in the net during deorbit. In addition, the nets are indifferent to the shapes and sizes of the objects in a wide range of parameters. Details will have to be discussed in a separate publication.

The electrodynamic vehicle specialized for wholesale debris removal from LEO was unveiled at the NASA-DARPA International Conference on Orbital Debris

Removal in 2009 [18]. We called it ElectroDynamic Debris Eliminator (EDDE). A dozen such vehicles launched on one ESPA ring (2 per slot) would be able to remove all objects over 2 kg from LEO (approximately 2,500 objects totaling 2,200 tons) in less than 7 years. A simulation showing this process can be viewed on the Web [24]. The overall efficiency is consistent with the predictions of Fig. 6. On average, each 100-kg vehicle can remove its own mass in debris every day, or up to 36 tons per year. It takes only 4 vehicles and 7 years to remove all upper stages from the 71-74°, 81-83°, and Sun-sync clusters and reduce the collision-generated debris potential in LEO by a factor of 4.

Economic analysis suggests that LEO debris removal as a commercial service could cost only a small fraction of typical launch costs per kilogram, making it affordable for the first time since the beginning of the space era. Wholesale removal of large debris with EDDE vehicles could cost around \$400/kg on average at the current prices. Also, a low-cost end-of-life retirement service could be provided to satellite operators in LEO to keep it clear of dead satellites and spent stages.

6. Collection and recycling

As an alternative to deorbit, many objects from crowded regions could be collected at intermediate altitudes for storage and possible future reuse. There are 1000 tons of old upper stages in LEO. Most of them are tightly clustered at high inclinations, and much of their mass is aluminum alloy tanks and related structure. Their recycling could provide a market mechanism for supporting debris removal [25]. If this market develops, each EDDE vehicle could deliver up to 30 tons of “scrap metal” per year to storage or in-orbit recycling facilities. Collection would also reduce risks associated with the reentry of many large objects during a wholesale removal campaign.

7. Traffic coordination

EDDE represents a new class of persistently maneuverable space vehicles that can move all over LEO constantly changing their orbits and performing a variety of jobs, such as removing orbital debris and delivering payloads. To navigate safely among other operational spacecraft and actively avoid all tracked objects in LEO, the EDDE operator would need a way to coordinate its flight plans with the Space Surveillance Network and take into account the plans of other spacecraft operators. A centralized flight plan coordination service, such as being developed by the Center for Space Standards and Innovation (CSSI), could support these operations in the future [26]. In addition, the debris removal vehicles can carry transponders and volunteer to broadcast their positions and velocities, based on GPS data, very much

like aircraft in the new ADS-B air traffic control system being deployed worldwide. This way, all interested parties will know at all times where is the communal “space garbage truck,” and there will be no surprises.

8. Conclusions

The task of wholesale debris removal is very challenging. It appears that neither drag devices nor rockets are well suited for it, and the only viable candidate with today’s technology is electrodynamic propulsion. It is propellantless, economic, and lightweight, but unorthodox. The electrodynamic vehicle of the latest design can be described as a set of nanosats on a string, but it can repeatedly move tons in LEO. Like a sailboat, it utilizes its natural environment (the geomagnetic field, ionospheric plasma, and solar power) to produce thrust, and like a sailboat, it needs certain dimensions to thrust efficiently. This may seem inconvenient, but if caravels were never built, we could have missed many opportunities and discoveries.

Electrodynamic propulsion technology has matured to the point where the vehicles can be made efficient and robust and provide a practical low-cost solution for wholesale LEO debris removal. A dozen electrodynamic vehicles launched as secondary payloads on ESPA can affordably remove nearly 2,500 objects of more than 2 kg totaling 2,200 tons from LEO in less than 7 years. That would remove more than 99% of the collision-generated debris potential in LEO. It would take only 4 vehicles and 7 years to remove all upper stages from the three main clusters, reducing the collision-generated debris potential by a factor of 4. There is no other vehicle that can match, or even remotely approach this performance today.

The estimated cost per kilogram of debris removed is a small fraction of typical launch costs per kilogram, making it possible to shift from debris mitigation to wholesale active removal of all large debris objects from LEO.

References

1. H. Klinkrad, Space Debris Mitigation Activities at ESA, February 2011.
2. D. J. Kessler, N.L. Johnson, J.-C. Liou, M. Matney, The Kessler Syndrome: Implications to Future Space Operations, AAS 10-016, Advances in the Astronautical Sciences, American Astronautical Society, v. 137, 2010, pp. 47-62.
3. H. Klinkrad, N.L. Johnson, Space Debris Environment Remediation Concepts, NASA-DARPA International Conference on Orbital Debris Removal, Chantilly, VA, December 8-10, 2009.
4. H. Klinkrad, N.L. Johnson, Mass Removal from Orbit: Incentives and Potential Solutions, 1st European Workshop on Active Debris Removal, July 22, 2010.

5. S. Fukushige, Y. Akahoshi, Y. Kitazawa, T. Goka, Comparison of Debris Environment Models: ORDEM2000, MASTER2001 and MASTER2005, IHI engineering review, v. 40, No. 1, 2007, pp. 31-41.
6. J. Carroll, Bounties for Orbital Debris Threat Reduction? NASA-DARPA International Conference on Orbital Debris Removal, Chantilly, VA, December 8-10, 2009.
7. J.-C. Liou, The Top 10 Questions for Active Debris Removal, 1st European Workshop on Active Debris Removal, July 22, 2010.
8. P. Demarest, The Debris Environment Around the Earth Science Morning and Afternoon Constellations, AIAA-2006-6292, AIAA/AAS Astrodynamics Specialist Conference and Exhibit, Keystone, CO, August 21-24, 2006.
9. Internet Database of Operational Satellites, http://www.ucsusa.org/satellite_database.
10. C. Bombardelli, J. Herrera-Montojo, A. Iturri-Torrea and J. Pelaez, Space Debris Removal with Bare Electrodynamic Tethers, AAS 10-270, AAS/AIAA Space Flight Mechanics Meeting, San Diego, CA, February 14-17, 2010.
11. Tether Applications Inc. Web Site, <http://www.tetherapplications.com>.
12. E.M. Levin, Dynamic Analysis of Space Tether Missions, Advances in the Astronautical Sciences, American Astronautical Society, v. 126, Univelt, 2007.
13. J. Pearson, J. Carroll, E. Levin, J. Oldson, P. Hausgen, Overview of the ElectroDynamic Delivery Express (EDDE), AIAA 2003-4790, 39th Joint Propulsion Conference, Huntsville, AL, July 21-13, 2003.
14. H.A. Fujii et al, Space Demonstration of Bare Electrodynamic Tape-Tether Technology on the Sounding Rocket S520-25, AIAA 2011-6503, AIAA Guidance, Navigation, and Control Conference, Portland, Oregon, August 8-11, 2011.
15. S. Kawamoto, Y. Ohkawa, S. Nishida, S. Kitamura, S. Kibe, T. Hanada, M. Mine, Strategies and Technologies for Cost Effective Removal of Large Sized Debris, NASA-DARPA International Conference on Debris Removal, Chantilly, VA, December 8-10, 2009.
16. S. Coffey, B. Kelm, A. Hoskins, J. Carroll, E. Levin, Tethered Electrodynamic Propulsion CubeSat Experiment (TEPCE), Air Force Orbital Resources Ionosphere Conference, Dayton, Ohio, January 12-14, 2010.
17. NRL Programs, TEPCE, <http://www.nrl.navy.mil/code8200/programs.php>.
18. J. Pearson, J. Carroll, E. Levin, J. Oldson, EDDE: ElectroDynamic Debris Eliminator for Active Debris Removal, NASA-DARPA International Conference on Orbital Debris Removal, Chantilly, VA, December 8-10, 2009.
19. E. J. van der Heide, M. Kruijff, Tethers and Debris Mitigation. Acta Astronautica, v. 48, No. 5-12, March-June 2001, pp. 503-516.
20. C. Pardini, T. Hanada, P.H. Krisko, Benefits and Risks of Using Electrodynamic Tethers to De-orbit Spacecraft, Acta Astronautica v. 64, No. 5-6, March-April 2009, pp. 571-588.
21. V. Williams and A.J. Meadows, Eddy Current Torques, Air Torques, and the Spin Decay of Cylindrical Rocket Bodies in Orbit, Planetary and Space Science, 1978, v.26, No.8,

pp.721-726.

22. C. Bonnal, Two Actions at IADC Level: Space Debris Movement Observation and Acceptability of Random Reentry of Large Debris, Ariadna Workshop, ESTEC, Noordwijk, Netherlands, June 10, 2011.

23. J.A. Carroll, Space Transport Development Using Orbital Debris, Final Report on NIAC Phase I, Research Grant No. 07600-087, December 2, 2002.

24. EDDE Debris Removal Simulation, <http://www.star-tech-inc.com/id121.html>.

25. J. Pearson, J. Carroll, E. Levin, J. Oldson, Electro Dynamic Debris Eliminator (EDDE) Opens LEO for Aluminum Recovery and Reuse. 14th Space Manufacturing Conference, NASA Ames, Sunnyvale, CA, October 30-31, 2010.

26. J. Pearson, E. Levin, J. Carroll, J. Oldson, ElectroDynamic Debris Eliminator (EDDE): Design, Operation, and Ground Support, 2010 AMOS Conference Proceedings, September 14-17, 2010, pp. 628-636.